VERIZONA PUBLISHER
Publishing Your Ideas

www.verizonaonlinepublishing.com
Vol: 1, Issue: 2

Journal of Robotics and Mechanical Engineering Research

Free Vibration of Circular Plates with Various Edge Boundary Conditions by 3-D Elasticity Theory

WD Tseng[1*], JQ Tarn[2], LY Tung[2], WY Liang[2]

[1]Department of Construction Engineering, Nan Jeon University of Science and Technology, Tainan, Taiwan
[2]Department of Civil Engineering, National Cheng Kung University, Tainan, Taiwan

***Corresponding author:** WD Tseng, Department of Construction Engineering, Nan Jeon University of Science and Technology, Tainan, Taiwan; Email: wdtseng1125@gmail.com

Article Type: Research, **Submission Date**: 17 June 2015, **Accepted Date:** 17 July 2015, **Published Date:** 08 August 2015.

Citation: WD Tseng, JQ Tarn, LY Tung, WY Liang (2015) Free Vibration of Circular Plates with Various Edge Boundary Conditions by 3-D Elasticity Theory. J Robot Mech Eng Resr 1(2): 28-35.

Abstract

Free vibration of transversely isotropic circular plates with various edge boundary conditions is analyzed on the basis of theory of elasticity without a priori plate assumptions. The governing equations for vibration of transversely isotropic circular plates are derived from the three-dimensional equations of elasticity in the cylindrical coordinates. By means of separation of variables, two sets of solutions are obtained, which enable us to satisfy various edge boundary conditions of the problems and determine the natural frequencies of the circular plates. Numerical results for three kinds of edge conditions are evaluated and compared with those obtained according to 2D plate theories such as DQM, HSDT and Mindlin's solutions. The study shows that our results can find much more natural frequencies of circular plates than the 2D solutions for circular plates. These 2D solutions are applicable while the ratios of thickness to radius of the plates are lesser than 0.05 and the edge conditions are clamped or simply-supported.

Keywords: Circular plates, Elasticity, Free vibration, Natural frequency.

Introduction

In the literature, considerable studies have been reported on the vibration analysis of plates. According to the classical 2D theory of flexural motion of elastic plates (CPT), the axial shear strains and normal stress have been neglected. Hence CPT cannot be expected to give good results for the high-order modes of natural frequencies. Mindlin [1] considered the influence of rotatory inertia and shear on isotropic plates and derived a more comprehensive 2D theory (first-order shear deformation plate theory, FSDT) which is analogous to Timoshenko's theory for bars. Mindlin's theory satisfies constitutive relations for transverse shear stresses and shear strains by using shear correction factor. The value of this factor is not unique but depends on the material, geometry, loading and boundary conditions. Recently, Liew *et al.* [2] had used the differential quadrature method (DQM) to analyze circular Mindlin's plates. But both CPT and FSDT cannot satisfied all the equations of elasticity and consider only the deflections of middle planes of plates.

The 2D elasticity solutions play important role in validation of results of thick plate theories. Reddy's simplified higher order theories (HSDT) [3] gave a parabolic variation of transverse shear stress through the thickness of the plate satisfying the shear stress free boundary conditions on the top and bottom surfaces of the plate. Thus, it does not require the shear correction factor. And Hosseini-Hashemi *et al.* [4] had used HSDT to establish exact closed-form frequency equations for thick circular plates. Besides the 2D elasticity solutions, there are a few articles which studied the vibrations of circular cylinders by using the numerical methods. For examples, Leissa and So [5] presented the resonance frequencies of elastic solid cylinders with various length to radius ratios and Poisson's ratios using the Ritz method. To analyze the free vibration of anisotropic cylinders, Heyliger [6] used functions that individually exactly satisfy the axisymmetric equations of motion in conjunction with the Ritz method. And Buchanan and Chua [7] studied isotropic and anisotropic cylinders using the finite element method.

Hutchinson [8] developed a series solution of the general 3D equations of elasticity and used it to find natural frequencies for the vibrations of solid elastic cylinders with traction-free surfaces. The method of solution involves combining exact solutions of the governing equations in three series which term by term satisfy three of the six boundary conditions. The remaining three boundary conditions are satisfied by orthogonalization on the boundaries. Lusher and Hardy [9] used the same method to analyze transversely isotropic finite cylinders with stress free boundary conditions. Ebenezer [10] extended the method used by Hutchinson to determine the vibration responses of isotropic solid cylinders to arbitrary distributions of stresses on the boundaries. Ding [11] proposed the exact solutions for free vibrations of transversely isotropic circular plates, but the edge conditions considered were limited to be slide-contact and elastic-supported.

In this work, a method is presented for calculating the natural frequencies for vibrations of transversely isotropic circular plates with various thickness to radius ratios and edge conditions. The axial and radial displacements are expressed as a sum of two infinite series. One series contains Bessel functions that form a complete set in the radial direction and another contains Fourier functions that form a complete set in the axial direction. Each term in both the series is an exact solution to the governing equations of displacements and has coefficients that are used to satisfy boundary and edge conditions. The stresses are also expressed in terms of complete sets of functions by using the expression for displacement. The coefficients in the series are determined by using the orthogonal properties of the functions to satisfy the boundary and edge conditions. Numerical results are presented to illustrate the natural frequencies of transversely isotropic circular plates. The results are compared with those obtained according to the Mindlin and HSDT plate theories, and the applicability of those 2D methods is also discussed.

Formulation of Problem

Since the displacement and traction BC can be expressed directly by the displacement vector $\mathbf{u}$ and the stress vectors σ_i (where the indices $i=1,2,3$ stand for r,θ,z, respectively), we reformulate the basic equations of anisotropic elasticity in cylindrical coordinates [12] in terms of these vectors and obtain the following a system of 2nd-order partial differential equations for $\mathbf{u}$:

$$\left(\begin{bmatrix} r\partial_r & \mathbf{K}+\partial_\theta \mathbf{I} & r\partial_z \end{bmatrix} \begin{bmatrix} \mathbf{C}_1 & \mathbf{C}_2 & \mathbf{C}_3 \\ \mathbf{C}_2 & \mathbf{C}_2 & \mathbf{C}_3 \\ \mathbf{C}_3 & \mathbf{C}_3 & \mathbf{C}_3 \end{bmatrix} \begin{bmatrix} r\mathbf{I}\partial_r \\ \mathbf{K}+\mathbf{I}\partial_\theta \\ r\mathbf{I}\partial_z \end{bmatrix} - r\rho\,\partial_t \right)\mathbf{u}=\mathbf{0}. \quad (1)$$

Where

$\mathbf{u}=[u_r \quad u_\theta \quad u_z]^T$, $\sigma_i=[\sigma_{ri} \quad \sigma_{\theta i} \quad \sigma_{zi}]^T$, the superscript T denotes the transpose, u_i are the displacement components and σ_{ij} are the stress components; ∂_r, ∂_θ, ∂_z denote partial differentiation with respect to r, θ and z, respectively, $\mathbf{I}$ is the identity matrix;

$$\mathbf{K}=\begin{bmatrix} 0 & -1 & 0 \\ 1 & 0 & 0 \\ 0 & 0 & 0 \end{bmatrix}, \quad \mathbf{K}^T=-\mathbf{K} \quad \mathbf{C}_j=\begin{bmatrix} c_{1i1j} & c_{1i2j} & c_{1i3j} \\ c_{2i1j} & c_{2i2j} & c_{2i3j} \\ c_{3i1j} & c_{3i2j} & c_{3i3j} \end{bmatrix},$$

c_{ijkl} are the 21 elastic constants in cylindrical coordinates; ρ is the mass density of the medium; ∂_t denote partial differentiation with respect to the time t. The solutions of these equations will contain integration constants which should be determined from displacements or stresses which may be prescribed at the curved and flat boundaries of the cylinder.

Consider an elastic circular plate of radius a and thickness h. Let us locate the origin of the cylindrical coordinates (r,θ,z) at the center of plate. With z axis being the axis of symmetry, the boundary conditions on the bottom plane at $z=-h/2$ and the upper plane at $z=h/2$ are traction-free:

$$[\sigma_{rz} \quad \sigma_{\theta z} \quad \sigma_{zz}]_{z=\pm h/2}=[0 \quad 0 \quad 0] \quad (2)$$

The edge conditions at $r=a$ are traction-free or clamped or their combination. Specifically,

(1) Clamped:

$$[u_r \quad u_\theta \quad u_z]_{r=a}=[0 \quad 0 \quad 0] \quad (3)$$

(2) Simply-supported:

$$[\sigma_{rr} \quad \sigma_{r\theta} \quad u_z]_{r=a}=[0 \quad 0 \quad 0]. \quad (4)$$

(3) Traction-free:

$$[\sigma_{rr} \quad \sigma_{r\theta} \quad \sigma_{rz}]_{r=a}=[0 \quad 0 \quad 0]. \quad (5)$$

Steady-State Harmonic Response of Circular Plate

By using the following non-dimensional parameters:

$$R=r/a, \quad Z=z/h, \quad \varepsilon=h/a, \quad (6)$$

$$\bar{u}_r=u_r/h, \quad \bar{u}_\theta=u_\theta/h, \quad \bar{u}_z=u_z/h, \quad \tau_j=\sigma_j/c_{11}, \quad (7)$$

we consider the steady-state harmonic vibration of a circular plate and seek the solution to Eq. (1) in the form

$$\begin{bmatrix} \bar{u}_r \\ \bar{u}_\theta \\ \bar{u}_z \end{bmatrix}=\begin{bmatrix} u_r^*(R,Z)\cos n\theta \\ u_\theta^*(R,Z)\sin n\theta \\ u_z^*(R,Z)\cos n\theta \end{bmatrix} e^{i\omega t}, \quad (8)$$

where ω is the natural frequency to be determined; $u_r^*(R,Z)$, $u_\theta^*(R,Z)$, and $u_z^*(R,Z)$ are functions of the spatial variables.

Solution by means of eigenfunction expansion requires determining the eigenvalues and eigenfunctions that satisfy homogeneous state equation and homogeneous BC in either r or z coordinate and deriving the orthogonality of the eigenvectors. Here we propose a method which does not require determining the eigensolution.

Consider first the case of the "even" solution in which the in-plane displacements $u_r^*(R,Z)$ and $u_\theta^*(R,Z)$ are symmetrical to the middle plane of the plate.

Solution in form of Fourier- Bessel series

First, we seek the solution in the form of Fourier- Bessel series:

$$\begin{bmatrix} u_r^*(R,Z) \\ u_\theta^*(R,Z) \\ u_z^*(R,Z) \end{bmatrix}_1=\sum_{m=0}^{\infty}\begin{bmatrix} [U_{m1}I_{n-1}(\lambda_m R)+U_{m2}I_{n+1}(\lambda_m R)]\cos\mu_m Z \\ [V_{m1}I_{n-1}(\lambda_m R)+V_{m2}I_{n+1}(\lambda_m R)]\cos\mu_m Z \\ W_m I_n(\lambda_m R)\sin\mu_m Z \end{bmatrix}, \quad (9)$$

where $\mu_m=2m\pi$; U_{nmi}, V_{nmi} $(i=1,2)$ and W_{nm} are unknown constants; I_n is the modified Bessel function of the first kind of order n; λ_m is a parameter to be determined.

Substituting Eq. (9) in Eq. (1), after manipulation using the derivative formulas of Bessel functions [13], we arrive at

$$U_{nm1}=U_{nm2}=-V_{nm1}=V_{nm2}=-\frac{1}{2}(c'_{44}+c'_{13})\lambda_{mk}\mu_m\varepsilon, \quad (10)$$

$$W_{nm}=c'_{11}\lambda_{mk}^2\varepsilon^2-c'_{44}\mu_m^2+\varpi^2, \quad (k=1,2) \quad (11)$$

with $c'_{ij}=c_{ij}/c_{11}$ and the non-dimensional frequency parameter to be determined:

$$\varpi=\sqrt{\rho/c_{11}}\,\omega h.$$

$$\lambda_{m1}=\frac{1}{\varepsilon}\sqrt{\frac{-\chi_{1m}+\sqrt{\chi_{1m}^2-\chi_{2m}}}{2c'_{11}c'_{44}}}, \quad \lambda_{m2}=\frac{1}{\varepsilon}\sqrt{\frac{-\chi_{1m}-\sqrt{\chi_{1m}^2-\chi_{2m}}}{2c'_{11}c'_{44}}},$$

$$\chi_{1m}=(-c'_{11}c'_{33}+2c'_{44}c'_{13}+c'_{13}c'_{13})\mu_m^2+(c'_{11}+c'_{44})\varpi^2,$$

$$\chi_{2m}=4c'_{11}c'_{44}(-c'_{44}\mu_m^2+\varpi^2)(-c'_{33}\mu_m^2+\varpi^2)$$

or

$$U_{m1} = -U_{m2} = -V_{m1} = -V_{m2}, \quad W_m = 0,$$

with

$$\lambda_{m3} = \frac{1}{\varepsilon}\sqrt{\frac{c'_4\,\mu_m^2 - \varpi^2}{c'_6}}. \tag{12}$$

To each μ_m there corresponds a solution of Eq. (9) determined within a constant. As a result,

$$\begin{bmatrix} u_r^*(R,Z) \\ u_\theta^*(R,Z) \\ u_z^*(R,Z) \end{bmatrix}_1 = a_0\begin{bmatrix} J_{n-1}(\lambda_{01}R) - J_{n+1}(\lambda_{01}R) \\ -J_{n-1}(\lambda_{01}R) - J_{n+1}(\lambda_{01}R) \\ 0 \end{bmatrix} + b_0\begin{bmatrix} J_{n-1}(\lambda_{03}R) + J_{n+1}(\lambda_{03}R) \\ -J_{n-1}(\lambda_{03}R) + J_{n+1}(\lambda_{03}R) \\ 0 \end{bmatrix} + \sum_{m=1}^{\infty}\sum_{k=1}^{2} a_{mk}\begin{bmatrix} A_{mk}[I_{n-1}(\lambda_{mk}R) + I_{n+1}(\lambda_{mk}R)]\cos\mu_m Z \\ -A_{mk}[I_{n-1}(\lambda_{mk}R) - I_{n+1}(\lambda_{mk}R)]\cos\mu_m Z \\ B_{mk} I_n(\lambda_{mk}R)\sin\mu_m Z \end{bmatrix} + \sum_{m=1}^{\infty} b_m\begin{bmatrix} [I_{n-1}(\lambda_{m3}R) - I_{n+1}(\lambda_{m3}R)]\cos\mu_m Z \\ -[I_{n-1}(\lambda_{m3}R) + I_{n+1}(\lambda_{m3}R)]\cos\mu_m Z \\ 0 \end{bmatrix}, \tag{13}$$

$$\begin{bmatrix} \tau_{rz}^*(R,Z) \\ \tau_{\theta z}^*(R,Z) \\ \tau_{zz}^*(R,Z) \end{bmatrix}_1 = a_0\begin{bmatrix} 0 \\ 0 \\ -2c'_{13}\lambda_{01}\varepsilon J_n(\lambda_{01}R) \end{bmatrix} + \sum_{m=1}^{\infty}\sum_{k=1}^{2} a_{mk}\begin{bmatrix} C_{mk}[I_{n-1}(\lambda_{mk}R) + I_{n+1}(\lambda_{mk}R)]\sin\mu_m Z \\ -C_{mk}[I_{n-1}(\lambda_{mk}R) - I_{n+1}(\lambda_{mk}R)]\sin\mu_m Z \\ D_{mk} I_n(\lambda_{mk}R)\cos\mu_m Z \end{bmatrix} + \sum_{m=1}^{\infty} b_m\begin{bmatrix} -c'_{44}\mu_m[I_{n-1}(\lambda_{m3}R) - I_{n+1}(\lambda_{m3}R)]\sin\mu_m Z \\ c'_{44}\mu_m[I_{n-1}(\lambda_{m3}R) + I_{n+1}(\lambda_{m3}R)]\sin\mu_m Z \\ 0 \end{bmatrix} \tag{14}$$

$$\begin{bmatrix} \tau_{rr}^*(R,Z) \\ \tau_{r\theta}^*(R,Z) \\ \tau_{\theta\theta}^*(R,Z) \end{bmatrix}_1 = a_0\begin{bmatrix} -2c'_{11}\lambda_{01}\varepsilon J_n(\lambda_{01}R) + \varepsilon M_0(\lambda_{01}R) \\ \varepsilon M_0^*(\lambda_{01}R) \\ -2c'_{12}\lambda_{01}\varepsilon J_n(\lambda_{01}R) - \varepsilon M_0(\lambda_{01}R) \end{bmatrix} + b_0\begin{bmatrix} 2c'_{66}\varepsilon R^{-1}N_0(\lambda_{03}R) \\ 2c'_{66}\varepsilon R^{-1}N_0^*(\lambda_{03}R) \\ -2c'_{66}\varepsilon R^{-1}N_0(\lambda_{03}R) \end{bmatrix} + \sum_{m=1}^{\infty}\sum_{k=1}^{2} a_{mk}\begin{bmatrix} [E_{mk}I_n(\lambda_{mk}R) + \varepsilon A_{mk}M_{mk}(\lambda_{mk}R)]\cos\mu_m Z \\ -\varepsilon A_{mk}M_{mk}^*(\lambda_{mk}R)\cos\mu_m Z \\ [F_{mk}I_n(\lambda_{mk}R) - \varepsilon A_{mk}M_{mk}(\lambda_{mk}R)]\cos\mu_m Z \end{bmatrix} + \sum_{m=1}^{\infty} b_m\begin{bmatrix} 2c'_{66}\varepsilon R^{-1}N_m(\lambda_{m3}R)\cos\mu_m Z \\ -2c'_{66}\varepsilon R^{-1}N_m(\lambda_{m3}R)\cos\mu_m Z \\ -2c'_{66}\varepsilon R^{-1}N_m(\lambda_{m3}R)\cos\mu_m Z \end{bmatrix} \tag{15}$$

where a_0, a_{mk} and b_m are constants to be determined; the known constants and functions are

$$\begin{bmatrix} A_{mk} \\ B_{mk} \\ C_{mk} \\ D_{mk} \\ E_{mk} \\ F_{mk} \end{bmatrix} = \begin{bmatrix} -\frac{1}{2}(c'_{11}+c'_{44})\varepsilon\lambda_{mk}\mu_m \\ c'_{11}\varepsilon^2\lambda_{mk}^2 - c'_{44}\mu_m^2 + \varpi^2 \\ \frac{1}{2}c'_{44}\varepsilon\lambda_{mk}(c'_{11}\varepsilon^2\lambda_{mk}^2 + c'_{13}\mu_m^2 + \varpi^2) \\ -\mu_m[c'_{13}(c'_{13}+c'_{44})\varepsilon^2\lambda_{mk}^2 - c'_{33}(c'_{11}\varepsilon^2\lambda_{mk}^2 - c'_{44}\mu_m^2 + \varpi^2)] \\ 2c'_{11}\varepsilon\lambda_{mk}A_{mk} + c'_{13}\mu_m B_{mk} \\ 2c'_{12}\varepsilon\lambda_{mk}A_{mk} + c'_{13}\mu_m B_{mk} \end{bmatrix},$$

$$\begin{bmatrix} M_0(\lambda_{01}R) \\ M_0^*(\lambda_{01}R) \\ M_{mk}(\lambda_{mk}R) \\ M_{mk}^*(\lambda_{mk}R) \end{bmatrix} = \begin{bmatrix} 2c'_{66}R^{-1}[(n-1)J_{n-1}(\lambda_{01}R) + (n+1)J_{n+1}(\lambda_{01}R)] \\ 2c'_{66}R^{-1}[-(n-1)J_{n-1}(\lambda_{01}R) + (n+1)J_{n+1}(\lambda_{01}R)] \\ 2c'_{66}R^{-1}[(n-1)I_{n-1}(\lambda_{mk}R) - (n+1)I_{n+1}(\lambda_{mk}R)] \\ 2c'_{66}R^{-1}[(n-1)I_{n-1}(\lambda_{mk}R) + (n+1)I_{n+1}(\lambda_{mk}R)] \end{bmatrix},$$

$$\begin{bmatrix} N_0(\lambda_{03}R) \\ N_0^*(\lambda_{03}R) \\ N_m(\lambda_{m3}R) \\ N_m^*(\lambda_{m3}R) \end{bmatrix} = \begin{bmatrix} (n-1)J_{n-1}(\lambda_{03}R) - (n+1)J_{n+1}(\lambda_{03}R) \\ \lambda_{03}RJ_n(\lambda_{03}R) - (n-1)J_{n-1}(\lambda_{03}R) - (n+1)J_{n+1}(\lambda_{03}R) \\ (n-1)I_{n-1}(\lambda_{m3}R) + (n+1)I_{n+1}(\lambda_{m3}R) \\ \lambda_{m3}RI_n(\lambda_{m3}R) + (n-1)I_{n-1}(\lambda_{m3}R) - (n+1)I_{n+1}(\lambda_{m3}R) \end{bmatrix}.$$

Solution in form of Fourier exponential series

Secondly, we seek the solution in the form of Fourier exponential series:

$$\begin{bmatrix} u_r^*(R,Z) \\ u_\theta^*(R,Z) \\ u_z^*(R,Z) \end{bmatrix}_2 = \sum_{p=1}^{\infty}\begin{bmatrix} U_p\,\exp(\mu_p Z)[J_{n-1}(\lambda_p R) - J_{n+1}(\lambda_p R)] \\ V_p\,\exp(\mu_p Z)[J_{n-1}(\lambda_p R) + J_{n+1}(\lambda_p R)] \\ W_p\,\exp(\mu_p Z)J_n(\lambda_p R) \end{bmatrix}, \tag{16}$$

where J_n is the Bessel function of the first kind of order n; λ_p is the root of $J_n(\lambda_p)=0$; U_{np}, V_{np} and W_{np} are unknown constants; μ_p is a parameter to be determined.

Substituting Eq. (16) in Eq. (1), after manipulation using the derivative formulas of Bessel functions, we arrive at

$$U_{np} = -V_{np} = \frac{1}{2}(c'_{44}+c'_{13})\lambda_p\mu_{pk}\varepsilon, \quad W_{np} = c'_{11}\lambda_p^2\varepsilon^2 - c'_{44}\mu_{pk}^2 - \varpi^2, \tag{17}$$

where $k = 1,2$;

$$\mu_{p1} = -\mu_{p3} = \sqrt{\frac{-\chi_{1p} + \sqrt{\chi_{1p}^2 - \chi_{2p}}}{2c'_{33}c'_{44}}}, \quad \mu_{p2} = -\mu_{p4} = \sqrt{\frac{-\chi_{1p} - \sqrt{\chi_{1p}^2 - \chi_{2p}}}{2c'_{33}c'_{44}}},$$

$$\chi_{1p} = (-c'_{11}c'_{33} + 2c'_{44}c'_{13} + c'_{13}c'_{13})\varepsilon^2\lambda_p^2 + (c'_{33}+c'_{44})\varpi^2,$$

$$\chi_{2p} = 4c'_{33}c'_{44}(-c'_{11}\varepsilon^2\lambda_p^2 + \varpi^2)(-c'_{44}\varepsilon^2\lambda_p^2 + \varpi^2)$$

To each λ_p there corresponds a solution of Eq. (9) determined within a constant. As a result,

$$\begin{bmatrix} u_r^*(R,Z) \\ u_\theta^*(R,Z) \\ u_z^*(R,Z) \end{bmatrix}_2 = \sum_{p=1}^{\infty}\sum_{l=1}^{2}\begin{bmatrix} (d_{pl}\sinh\mu_{pl}Z + f_{pl}\cosh\mu_{pl}Z)F_{pl}[J_{n-1}(\lambda_p R) - J_{n+1}(\lambda_p R)] \\ -(d_{pl}\sinh\mu_{pl}Z + f_{pl}\cosh\mu_{pl}Z)F_{pl}[J_{n-1}(\lambda_p R) + J_{n+1}(\lambda_p R)] \\ (d_{pl}\cosh\mu_{pl}Z + f_{pl}\sinh\mu_{pl}Z)G_{pl}J_n(\lambda_p R) \end{bmatrix} \tag{18}$$

$$\begin{bmatrix} \tau_{rz}^*(R,Z) \\ \tau_{\theta z}^*(R,Z) \\ \tau_{zz}^*(R,Z) \end{bmatrix}_2 = \sum_{p=1}^{\infty}\sum_{l=1}^{2}\begin{bmatrix} (d_{pl}\cosh\mu_{pl}Z + f_{pl}\sinh\mu_{pl}Z)H_{pl}[J_{n-1}(\lambda_p R) - J_{n+1}(\lambda_p R)] \\ -(d_{pl}\cosh\mu_{pl}Z + f_{pl}\sinh\mu_{pl}Z)H_{pl}[J_{n-1}(\lambda_p R) + J_{n+1}(\lambda_p R)] \\ (d_{pl}\sinh\mu_{pl}Z + f_{pl}\cosh\mu_{pl}Z)L_{pl}J_n(\lambda_p R) \end{bmatrix}. \tag{19}$$

$$\begin{bmatrix} \tau_{rr}^*(R,Z) \\ \tau_{r\theta}^*(R,Z) \\ \tau_{\theta\theta}^*(R,Z) \end{bmatrix}_2 = \sum_{p=1}^{\infty}\sum_{l=1}^{2}\begin{bmatrix} (d_{pl}\sinh\mu_{pl}Z + f_{pl}\cosh\mu_{pl}Z)[K_{pl}J_n(\lambda_p R) + 2c'_{66}\varepsilon R^{-1}F_{pl}Q_n(\lambda_p R)] \\ -2c'_{66}\varepsilon R^{-1}F_{pl}(d_{pl}\sinh\mu_{pl}Z + f_{pl}\cosh\mu_{pl}Z)Q_n^*(\lambda_p R) \\ (d_{pl}\sinh\mu_{pl}Z + f_{pl}\cosh\mu_{pl}Z)[K_{pl}J_n(\lambda_p R) - 2c'_{66}\varepsilon R^{-1}F_{pl}Q_n(\lambda_p R)] \end{bmatrix} \tag{20}$$

where d_{pl} is a constant to be determined; the known constants and functions are

$$\begin{bmatrix} F_{pl} \\ G_{pl} \\ H_{pl} \\ K_{pl} \\ L_{pl} \end{bmatrix} = \begin{bmatrix} \frac{1}{2}(c'_{33}+c'_{44})\varepsilon\mu_{pl}\lambda_p \\ c'_{11}\varepsilon^2\lambda_p^2 - c'_{44}\mu_{pl}^2 - \varpi^2 \\ \frac{1}{2}c'_{44}\varepsilon\lambda_p(c'_{11}\varepsilon^2\lambda_p^2 + c'_{13}\mu_{pl}^2 - \varpi^2) \\ -\mu_{pl}[c'_{11}(c'_{13}+c'_{44})\varepsilon^2\lambda_p^2 - c'_{13}(c'_{11}\varepsilon^2\lambda_p^2 - c'_{44}\mu_{pl}^2 - \varpi^2)] \\ -\mu_{pl}[c'_{13}(c'_{13}+c'_{44})\varepsilon^2\lambda_p^2 - c'_{33}(c'_{11}\varepsilon^2\lambda_p^2 - c'_{44}\mu_{pl}^2 - \varpi^2)] \end{bmatrix},$$

$$\begin{bmatrix} Q_n(\lambda_p R) \\ Q_n^*(\lambda_p R) \end{bmatrix} = \begin{bmatrix} (n-1)J_{n-1}(\lambda_p R) + (n+1)J_{n+1}(\lambda_p R) \\ (n-1)J_{n-1}(\lambda_p R) - (n+1)J_{n+1}(\lambda_p R) \end{bmatrix}.$$

Satisfaction of the BC at *z*=±*h*/2

Combining two sets of solution in Eqs. (13)-(15) and in (18)-(20), we obtain a solution in which the first series is Fourier-Bessel series with exponential power $\mu_m Z$ and argument $\lambda_{mk}R$; the second one is Fourier-Bessel series with argument $\lambda_p R$ and exponential power $\mu_{pl}Z$. While either series alone does not satisfy all the BC, the two series solutions together are made to satisfy the BC of the problem.

To this end, imposing the BC in the *z* direction yields a Fourier-Bessel series with argument $\lambda_p R$ and a series with argument $\lambda_{mk}R$. Upon representing the prescribed functions in *R* at the boundary planes and the series with argument $\lambda_{mk}R$ in Fourier-Bessel series with argument $\lambda_p R$ to make them compatible, the unknown constants in the series can be determined by comparing the coefficients in an elementary way.

Thus imposing the traction-free BC, Eqs. (2), at *z*=±*h*/2 on the relevant stress components in Eqs. (14) and (19) leads to

$$a_0\begin{bmatrix}0\\0\\-2c'_{13}\lambda_{01}\varepsilon J_n(\lambda_{01}R)\end{bmatrix}+\sum_{m=1}^{\infty}\sum_{k=1}^{2}a_{mk}\begin{bmatrix}0\\0\\(-1)^m D_{mk}I_n(\lambda_{mk}R)\end{bmatrix}$$

$$+\sum_{p=1}^{\infty}\sum_{l=1}^{2}\begin{bmatrix}\left[d_{pl}\cosh\left(\frac{\pm\mu_{pl}}{2}\right)+f_{pl}\sinh\left(\frac{\pm\mu_{pl}}{2}\right)\right]H_{pl}\left[J_{n-1}(\lambda_pR)-J_{n+1}(\lambda_pR)\right]\\-\left[d_{pl}\cosh\left(\frac{\pm\mu_{pl}}{2}\right)+f_{pl}\sinh\left(\frac{\pm\mu_{pl}}{2}\right)\right]H_{pl}\left[J_{n-1}(\lambda_pR)+J_{n+1}(\lambda_pR)\right]\\\left[d_{pl}\sinh\left(\frac{\pm\mu_{pl}}{2}\right)+f_{pl}\cosh\left(\frac{\pm\mu_{pl}}{2}\right)\right]L_{pl}J_n(\lambda_pR)\end{bmatrix}=\begin{bmatrix}0\\0\\0\end{bmatrix} \quad (21)$$

Eq. (21) can be decoupled into these equations:

$$-2c'_{13}\lambda_{01}\varepsilon J_n(\lambda_{01}R)a_0+\sum_{m=1}^{\infty}\sum_{k=1}^{2}a_{mk}(-1)^m D_{mk}I_n(\lambda_{mk}R)+\sum_{p=1}^{\infty}\sum_{l=1}^{2}f_{pl}L_{pl}\cosh\left(\frac{\mu_{pl}}{2}\right)J_n(\lambda_pR)=0, \quad (22)$$

$$\sum_{p=1}^{\infty}\sum_{l=1}^{2}d_{pl}H_{pl}\cosh\left(\frac{\mu_{pl}}{2}\right)\left[J_{n-1}(\lambda_pR)-J_{n+1}(\lambda_pR)\right]=0, \quad (23)$$

$$\sum_{p=1}^{\infty}\sum_{l=1}^{2}d_{pl}H_{pl}\cosh\left(\frac{\mu_{pl}}{2}\right)\left[J_{n-1}(\lambda_pR)+J_{n+1}(\lambda_pR)\right]=0, \quad (24)$$

$$\sum_{p=1}^{\infty}\sum_{l=1}^{2}d_{pl}L_{pl}\sinh\left(\frac{\mu_{pl}}{2}\right)J_n(\lambda_pR)=0, \quad (25)$$

$$\sum_{p=1}^{\infty}\sum_{l=1}^{2}f_{pl}H_{pl}\sinh\left(\frac{\mu_{pl}}{2}\right)\left[J_{n-1}(\lambda_pR)-J_{n+1}(\lambda_pR)\right]=0, \quad (26)$$

$$\sum_{p=1}^{\infty}\sum_{l=1}^{2}f_{pl}H_{pl}\sinh\left(\frac{\mu_{pl}}{2}\right)\left[J_{n-1}(\lambda_pR)+J_{n+1}(\lambda_pR)\right]=0, \quad (27)$$

which can be reduced to

$$d_{p1}=d_{p2}=0, \quad (28)$$

$$f_{p2}H_{p2}\sinh(m_{p2}/2)=f_{p1}H_{p1}\sinh(m_{p1}/2)=f_p, \quad (29)$$

and

$$-2c'_{13}\lambda_{01}\varepsilon J_n(\lambda_{01}R)a_0+\sum_{m=1}^{\infty}\sum_{k=1}^{2}a_{mk}(-1)^m D_{mk}I_n(\lambda_{mk}R)+\sum_{p=1}^{\infty}f_p\sum_{l=1}^{2}\left[\frac{L_{pl}}{H_{pl}}\frac{\cosh(\mu_{pl}/2)}{\sinh(\mu_{pl}/2)}\right]J_n(\lambda_pR)=0. \quad (30)$$

The functions $J_n(\lambda_{01}R)$ and $I_n(\lambda_{mk}R)$ in Eq. (30) can be expressed in terms of $J_n(l_pR)$:

$$J_n(\lambda_{01}R)=\sum_{p=1}^{\infty}\gamma_pJ_n(\lambda_pR), \quad I_n(\lambda_{mk}R)=\sum_{p=1}^{\infty}\phi_{pmk}J_n(\lambda_pR), \quad (31)$$

where

$$\gamma_p=\frac{2}{J_{n+1}^2(\lambda_p)}\int_0^1 RJ_n(\lambda_{01}R)J_n(\lambda_pR)dR,$$

$$\phi_{pmk}=\frac{2}{J_{n+1}^2(\lambda_p)}\int_0^1 RI_n(\lambda_{mk}R)J_n(\lambda_pR)dR.$$

For each $J_n(l_pR)$, the equation reduced from Eq. (30) is

$$-2c'_{13}\lambda_{01}\varepsilon\gamma_pa_0+f_pK_p+\sum_{m=1}^{\infty}\sum_{k=1}^{2}a_{mk}(-1)^mD_{mk}\phi_{pmk}=0, \quad (32)$$

Where

$$K_p=\sum_{l=1}^{2}\left[\frac{L_p}{H_p}\frac{\cosh(m_p/2)}{\sinh(m_p/2)}\right].$$

Eq. (32) can be rewritten as

$$f_p+\sum_{m=0}^{\infty}a_mX_{mp}=0, \quad (33)$$

where f_p and a_m are two kinds of unknown constants;

$$X_{0p}=-2c'_{13}\lambda_{01}\varepsilon(\gamma_p/K_p), \quad X_{mp}=\sum_{k=1}^{2}\frac{(-1)^mD_{mk}\phi_{pmk}}{K_pB_{mk}I_n(\lambda_{mk})}, \quad m\geq$$

Satisfaction of the BC at *r*=*a*

Likewise, imposing the BC in the radial direction yields a series in exponential power of $\mu_{pl}Z$ and a Fourier series in exponential power of μ_mZ. To make the two series compatible, it is necessary to express the prescribed functions in *z* at the boundary surfaces and the series with exponential power $\mu_{pl}Z$ in Fourier series with exponential power of μ_mZ, then the unknown constants in the series can be determined by comparing the coefficients.

According to Eqs. (3)-(5), the edge condition at *r*=*a* are traction-free or clamped or their combination.

Clamped BC at *r*=*a*: Imposing Eq. (3) on the relevant displacement components in Eqs. (13) and (18) leads to

$$a_0R_{01}+b_0S_{03}+\sum_{m=1}^{\infty}b_mR_{m3}\cos(\mu_mZ)+\sum_{m=1}^{\infty}\sum_{k=1}^{2}a_{mk}A_{mk}S_{mk}\cos(\mu_mZ)+\sum_{p=1}^{\infty}f_pT_p\sum_{l=1}^{2}\left[\frac{F_{pl}\cosh(\mu_{pl}Z)}{H_{pl}\sinh(\mu_{pl}/2)}\right]=0, \quad (34)$$

$$(a_0S_{01}+b_0R_{03})+\sum_{m=1}^{\infty}\left(b_mS_{m3}+\sum_{k=1}^{2}a_{mk}A_{mk}R_{mk}\right)\cos(\mu_mZ)=0, \quad (35)$$

$$\sum_{m=1}^{\infty}\sum_{k=1}^{2}a_{mk}B_{mk}I_n(\lambda_{mk})\sin(\mu_mZ)=0, \quad (36)$$

where

$$S_{0k}=J_{n-1}(\lambda_{0k})+J_{n+1}(\lambda_{0k}), \quad R_{0k}=J_{n-1}(\lambda_{0k})-J_{n+1}(\lambda_{0k}), \quad (k=1,3)$$

$$S_{mk}=I_{n-1}(\lambda_{mk})+I_{n+1}(\lambda_{mk}), \quad R_{mk}=I_{n-1}(\lambda_{mk})-I_{n+1}(\lambda_{mk}), \quad (m\geq1, \quad k=1,2,3)$$

$$T_p=J_{n-1}(\lambda_p)-J_{n+1}(\lambda_p)$$

From Eqs. (34)-(36) we have

$$b_0 = -a_0 \frac{S_{01}}{R_{03}}, \quad (37)$$

$$a_{m2} B_{m2} I_n(\lambda_{m2}) = a_{m1} B_{m1} I_n(\lambda_{m1}) = a_m, \quad (38)$$

$$b_m = -a_m \sum_{k=1}^{2} \frac{A_{mk}(R_{mk}/S_{m3})}{B_{mk} I_n(\lambda_{mk})}, \quad (39)$$

and

$$a_0 N_0 + \sum_{m=1}^{\infty} a_m N_m \cos(\mu_m Z) + \sum_{p=1}^{\infty} f_p T_p \sum_{l=1}^{2} \left[\frac{F_{pl}\cosh(\mu_{pl} Z)}{H_{pl}\sinh(\mu_{pl}/2)} \right] = 0, \quad (40)$$

where

$$N_0 = R_{01} - \frac{S_{01}}{R_{03}} S_{03}, \quad N_m = \sum_{k=1}^{2} \frac{A_{mk} S_{mk} - R_{mk}(R_{m3}/S_{m3})}{B_{mk} I_n(\lambda_{mk})}, \quad (m \ge 1).$$

The function $\cosh(\mu_{pl}Z)$ in Eq. (40) can be expressed in terms of $\cos(\mu_m Z)$:

$$\cosh(\mu_{pl} Z) = \varsigma_{pl0} + \sum_{m=1}^{\infty} \varsigma_{plm} \cos(\mu_m Z), \quad (41)$$

Where $\varsigma_{pl0} = 2\int_0^{1/2} \cosh(\mu_{pl} Z) dZ, \ \varsigma_{plm} = 4\int_0^{1/2} \cosh(\mu_{pl} Z)\cos(\mu_m Z) dZ.$

For each $\cos \mu_m Z$, the equation reduced from Eq. (40) can be written as

$$a_m + \sum_{p=1}^{\infty} f_p Y_{pm} = 0, \quad (42)$$

where

$$Y_{pm} = \frac{T_p}{N_m} \sum_{l=1}^{2} \frac{\varsigma_{plm}}{H_{pl}\sinh(\mu_{pl}/2)}, \quad (m \ge 0).$$

Simply supported BC at *r=a*: Likewise, imposing Eq. (4) on the relevant displacement and stress components in Eqs. (13)-(15) and (18)-(20) and then expressing the function $\cosh(\mu_{pl}Z)$ in terms of $\cos(\mu_m Z)$ leads to a set of equations like Eq. (42).

Traction-free BC at *r=1*: Likewise, imposing Eq. (5) on the relevant displacement components in Eqs. (14)-(15) and (19)-(20) and then expressing the function $\cosh(\mu_{pl}Z)$ And $\sinh(\mu_{pl} Z)$ in terms of $\cos(\mu_m Z)$ and $\sin(\mu_m Z)$, respectively, leads to a set of equations like Eq. (42).

Eq. (42) for clamped BC (or for simply-supported or traction-free BC) at *r=a* and Eq. (33) constitute a system of equations

$$f_p + \sum_{m=0}^{\infty} a_m X_{mp} = 0, \quad (43)$$

$$a_m + \sum_{p=1}^{\infty} f_p Y_{pm} = 0, \quad (44)$$

in which the unknowns are f_p and a_m. The boundary conditions only lead to the relationship between the undetermined constants. Thus, taking *N* terms of the two series for computation, we arrive at a system of 2*N* algebraic equations for the 2*N* unknowns (*m*=1,2,...,*N*, *p*=1,2,...,*N*), which has nontrivial solutions if and only if the determinant of the coefficient matrix is zero. This condition leads to a transcendental equation in terms of non-dimensional frequency parameter ϖ which can be determined by using a standard method for finding roots such as the bisection method. The solution process is to choose a value of ϖ and evaluate the determinant. If the determinant is zero, the value is one of the frequency parameters.

The case of the "odd" solution in which the in-plane displacements $u_r^*(R,Z)$ and $u_\theta^*(R,Z)$ are anti-symmetrical to the middle plane of the plate can be solved in a similar process like Sections 3.1-3.4 except the parameter μ_m being taken as $(2m-1)\pi$.

Results and Discussions

To examine quantitatively the natural frequency of steady-state harmonic vibration in circular plates, we consider the axisymmetric case for simplicity and take c_{33}/c_{11}= 5, 1, 3/4, 1/2, 1/3 and 1/4 for transversely isotropic materials. The ratios of thickness to radius of the plates are taken to be *h*/*a*=0.001, 0.05, 0.1 and 0.2. For isotropic plates, Liew *et al.* [2] adopted the non-dimensional frequency parameter $\alpha = \sqrt{\rho h / D}\,\omega a^2$ where $D = Eh^3/\left[12(1-\nu)^2\right]$. The parameter ϖ of present analysis can be converted to α by using the relation $\alpha = \sqrt{12(1-\nu)^2/\left[\varepsilon^4(1-2\nu)\right]}\varpi$ and compared with those of DQM [2] and Hosseini-Hashemi's HSDT [4] results. For transversely isotropic plates, we use the non-dimensional frequency parameter $\beta = \varepsilon\varpi$ to present our results. And for comparison, the parameters β have also been calculated from Mindlin's solution for circular plates [11].

In evaluating the natural frequency, Tables 1-3 display the results of *h*/*a*=0.001 for isotropic plates under three kinds of edge conditions by taking 5, 10, 15 and 20 terms of the series for computation. The tabulated values are the lowest five frequency parameters and show the convergences of the frequencies.

Table 1: α of *h*/*a*=0.001 for isotropic materials at clamped edges

Terms	Mode				
	1	2	3	4	5
5	10.2245	39.1000	87.9500	159.5000	245.4000
10	10.0870	39.7477	88.6000	159.5000	245.4000
15	10.1690	39.3250	88.6025	157.7500	245.8500
20	10.2375	39.2972	89.2750	158.2915	246.9500

Table 2: α of *h*/*a*=0.001 for isotropic materials at simply-supported edges

Terms	Mode				
	1	2	3	4	5
5	5.0519	29.8687	74.2334	138.3771	222.2378
10	5.0841	29.8597	74.2215	138.9977	222.3721
15	4.9000	29.8041	74.2162	138.1594	222.2155
20	4.9300	29.6302	74.2131	138.3528	222.2123

Table 3: α of *h*/*a*=0.001 for isotropic materials at traction-free

edges

Terms	Mode				
	1	2	3	4	5
5	8.9499	36.4514	83.4004	140.1872	244.4387
10	8.9506	38.2400	86.9795	157.0156	244.4500
15	8.9506	38.2509	86.9795	156.9983	245.3999
20	8.9508	38.2509	87.0039	156.9362	245.4110

As shown in Figure 1 for traction-free edge conditions, the solutions converge as more terms in the series are chosen and taking about 10 terms produce excellent results for the lower frequencies. The higher mode parameters always converge slower. As the terms increase, the oscillating result is closer to a mean value. To achieve satisfactory convergence, it is necessary to take no lesser than 15 terms in each series for higher modes.

Tables 4-6 present the frequency parameters a obtained using 20 terms in each series and of various h/a for isotropic plates under three kinds of edge conditions. In these tables the results obtained by DQM and HSDT are also presented for comparison. It is found that the frequency parameters decrease as h/a increases. And the comparisons show that the DQM and HSDT results are closer to those of the present solutions when the value of h/a is between 0.05 and 0.001. Especially for h/a equal to 0.001, the errors of frequency parameters of DQM and HSDT to present solution are under 3%. As h/a increases to 0.1~0.2, the error increases for higher modes. Since the 2D plate theory assumes that the axial deformation is very small and the axial normal stress can be neglected thus the equations of motion and both the top and bottom surface BC are not all satisfied, some higher frequencies even cannot be found for thicker plates by DQM and HSDT rather than the present results which consist of the "even" and "odd" modes stated in Section 3. As for the lateral boundary conditions, the errors of frequency parameters for thicker plates with traction-free edges are greatest among those of three kinds of BC. The clamped edge provides much stronger constraint to plate, so the natural frequencies are larger than the other two conditions. Since the real stress distributions are less uniform as h/a increases and the edge boundary conditions are relaxed and satisfied only in an average sense by DQM and HSDT, these two methods are not applicable while h/a is greater than 0.05 and the edge conditions are traction-free.

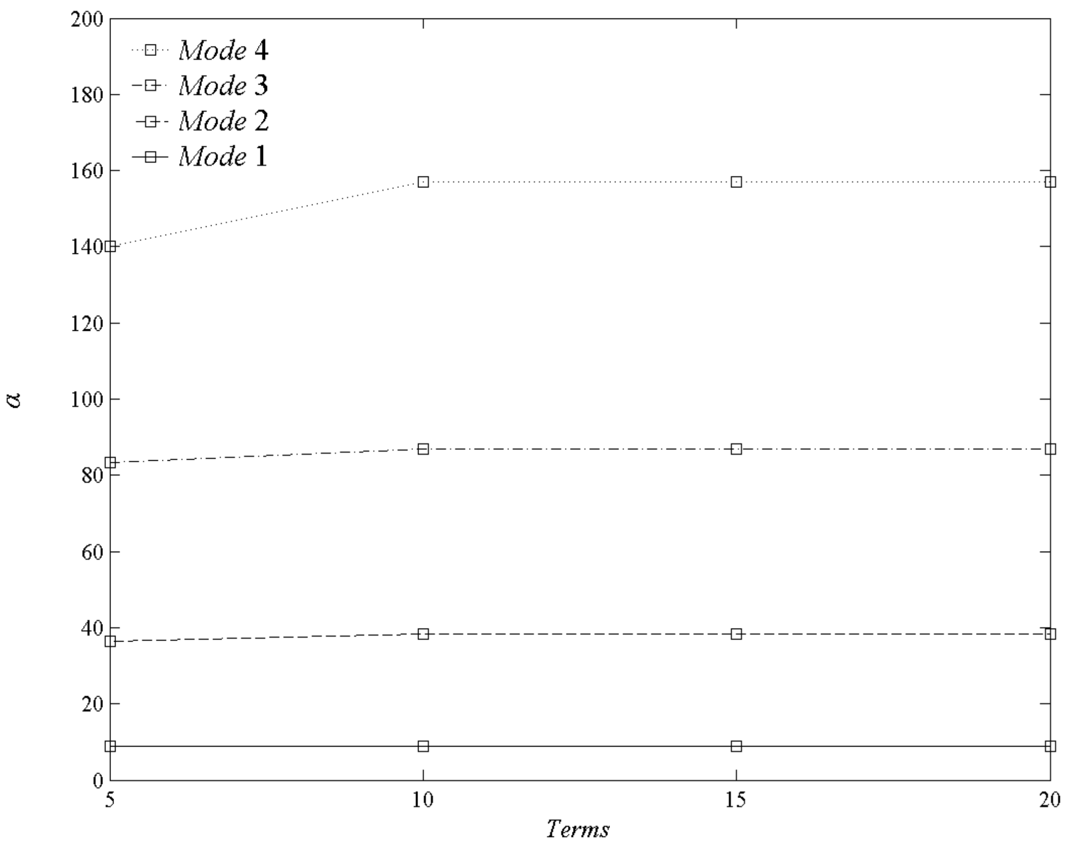

Figure1: Comparison of α of different modes and terms at traction-free edges

Table 4: Comparison of α of various h/a for isotropic materials at clamped edges

h/a	Method	Mode				
		1	2	3	4	5
0.001	Present	10.238	39.297	89.275	158.292	246.950
	HSDT	10.216	39.771	89.102	158.179	246.994
	DQM	10.216	39.771	89.102	158.180	246.990
0.05	Present	9.721	36.5340	72.4538	82.411	98.569
	HSDT	10.146	38.8706	-	84.995	-
	DQM	10.145	38.8550	-	84.995	-
0.1	Present	9.414	34.8754	49.2843	74.431	92.319
	HSDT	9.946	36.5489	-	75.954	-
	DQM	9.941	36.4790	-	75.664	-
0.2	Present	9.064	26.621	46.3461	51.030	74.817
	HSDT	9.265	30.475	-	57.533	-
	DQM	9.240	30.211	-	56.682	-

Tables 7-8 display the frequency parameters β obtained using 20 terms in each series and of h/a=0.001 and 0.05 for various transversely isotropic plates under simply-supported edge conditions. For weaker c_{33}/c_{11}, the natural frequencies are smaller and two adjacent frequencies are closer. Stronger c_{33}/c_{11} means much stronger resistance to deformation, the natural frequencies are larger. The results obtained by Mindlin's solutions are also included in these tables for comparison. It can be found that for h/a=0.001 and higher modes of frequency the results of Mindlin's solutions are closer to those of present solutions. The errors of frequency parameters of Mindlin's solution to present solution increase as c_{33}/c_{11} decrease. While c_{33}/c_{11} is 1/4, the first mode of Mindlin's solutions cannot be found for h/a=0.001 and 0.05. Thus the Mindlin's solutions are not applicable while c_{33}/c_{11} is less than 1/4.

Table 5: Comparison of α of various h/a for isotropic materials at simply-supported edges

h/a	Method	Mode				
		1	2	3	4	5
0.05	Present	4.906	29.366	71.579	126.470	142.417
	HSDT	4.925	29.327	71.780	130.429	-
	DQM	4.925	29.323	71.756	130.350	-
0.1	Present	4.876	28.210	49.284	62.957	72.088
	HSDT	4.894	28.255	-	66.024	-
	DQM	4.894	28.240	-	65.942	-
0.2	Present	4.786	24.648	35.182	53.857	56.564
	HSDT	4.779	25.041	-	52.739	-
	DQM	4.777	24.994	-	52.514	-

Table 6: Comparison of α of various h/a for isotropic materials at traction-free edges

h/a	Method	Mode				
		1	2	3	4	5
0.1	Present	4.8780	28.2333	49.2109	63.8099	72.4778
	HSDT	8.8688	36.0613	-	76.7776	-
	DQM	8.8679	36.0410	-	76.676	-
0.2	Present	4.7151	24.7682	36.4160	45.7227	57.2846
	HSDT	8.5084	-	31.1748	-	59.9152
	DQM	8.5051	-	31.1110	-	59.6450

Table 7: Comparison of β of h/a=0.001 and various c_{33}/c_{11} at simply-supported edges

c_{33}/c_{11}	Method	Mode			
		1	2	3	4
5	Present	1.4948	8.6101	21.2065	39.3864
	Mindlin	1.4414	8.4548	21.0425	39.2194
1	Present	1.2780	7.7349	19.3562	36.0767
	Mindlin	1.2872	7.7515	19.3411	36.0751
3/4	Present	1.2470	7.6121	18.7708	34.8694
	Mindlin	1.2166	7.4387	18.5861	34.6808
1/2	Present	1.0759	6.9586	17.1775	31.9150
	Mindlin	1.0594	6.7691	16.9753	31.7084
1/3	Present	0.7691	5.8456	14.4633	26.8820
	Mindlin	0.7516	5.6133	14.2187	26.6334
1/4	Present	0.3039	4.4703	11.1074	20.6587
	Mindlin	-	4.1280	10.7678	20.3207

Table 8: Comparison of β of h/a=0.05 and various c_{33}/c_{11} at simply-supported edges

c_{33}/c_{11}	Method	Mode			
		1	2	3	4
5	Present	1.4339	8.4684	20.4284	36.8528
	Mindlin	1.4372	8.3044	20.1460	36.2821
1	Present	1.2796	7.6592	18.6693	32.9859
	Mindlin	1.2840	7.6314	18.6171	33.6849
3/4	Present	1.2148	7.5145	18.2228	26.5812
	Mindlin	1.2138	7.3305	17.9309	32.5102
1/2	Present	1.0643	6.8851	16.7524	24.5547
	Mindlin	1.0574	6.6837	16.4516	29.9606
1/3	Present	0.7839	5.8032	14.2025	19.5120
	Mindlin	0.7506	5.5587	13.8756	-
1/4	Present	0.2940	4.4484	10.9782	14.3546
	Mindlin	-	4.0999	10.5818	-

Conclusions

An exact analysis of free vibration of circular elastic plates of transversely isotropic materials with various edge conditions has been developed. We can seek the 3D solution by using separation of variables and assume it as a sum of two infinite series. One series contains Fourier functions that form a complete set in the axial direction and another contains Bessel functions that form a complete set in the radial direction. Each term in both series is an exact solution to the governing equations and has a coefficient that is used to satisfy boundary conditions.

The study shows that our results can find much more natural frequencies of circular plates than DQM, HSDT and Mindlin's solutions for circular plates. As h/a is greater than 0.05 or the plates are under traction-free edge conditions, the errors of frequency parameter of DQM and HSDT solution to present solution increase and some higher modes of frequency cannot be found by these methods. And as c_{33}/c_{11} is less than 1/4, the errors of frequency parameter of Mindlin's solution to present solution increase and the first mode cannot be found by Mindlin's solutions. These 2D solutions are applicable while h/a is lesser than 0.05 and the edge conditions are clamped or simply-supported.

References

1. Mindlin RD. Influence of Rotatory Inertia and Shear on Flexural Motions of Isotropic elastic plates. Journal of Applied Mechanics. 1951; 18:31-38.
2. Liew KM, Han JB, Xiao ZM. Vibration Analysis of Circular Mindlin Plates Using The Differential Quadrature Method. Journal of Sound and Vibration. 1997; 205(5):617-630. doi:10.1006/jsvi.1997.1035.
3. Reddy JN. A Refined Nonlinear Theory of Plates with Transverse Shear Deformation, International. Journal of Solids and Structures. 1984; 20(9-10):881-896. doi: 10.1016/0020-7683(84)90056-8.
4. Hosseini-Hashemi S, Es'haghi M, Rokni Damavandi Taher H, Fadaie M. Exact Closed-form Frequency Equations for Thick Circular Plates Using A Third-order Shear Deformation Theory. Journal of Sound and Vibration. 2010; 329(16):3382-3396. doi:10.1016/j.jsv.2010.02.024.
5. Leissa AW, So J. Accurate Vibration Frequencies of Circular Cylinders from Three-dimensional Analysis. J. Acoust. Soc. Am. 1995; 98:2136–2141. doi: http://dx.doi.org/10.1121/1.414403.
6. Heyliger PR. Axisymmetric Free Vibrations of Finite Anisotropic Cylinders. Journal of Sound and Vibration. 1991; 148(3):507–520. doi:10.1016/0022-460X(91)90481-X
7. Buchanan GR, Chua CL. Frequencies and Mode Shapes for Finite Length Cylinders. Journal of Sound and Vibration. 2001; 246(5):927–941. doi: 10.1006/jsvi.2001.3620.
8. Hutchinson JR. Vibrations of Solid Cylinder. Journal of Applied Mechanics. 1980; 47:901-907.
9. Lusher CP, Hardy WN. Axisymmetric Free Vibrations of A Transversely Isotropic Finite Cylindrical Rod. Journal of Applied Mechanics. 1988; 55(4):855–862. doi: 10.1115/1.3173733.
10. Ebenezer DD, Ravichandran K, Padmanabhan C. Forced Vibrations of Solid Elastic Cylinders. Journal of Sound and Vibration. 2005; 282(3-5):991-1007. doi:10.1016/j.jsv.2004.03.070.
11. Ding HJ, Xu RQ. Exact Solutions for Free Vibrations of Transversely Isotropic Circular Plates. Acta Mechanica. 2000; 13:105-111.
12. Tarn JQ. A State Space Formalism for Anisotropic Elasticity. Part II: Cylindrical Anisotropy. *International Journal of Solids and Structures. 2002;* 39(20):5157-5172. doi:10.1016/S0020-7683(02)00412-2.
13. Hildebrand FB. *Advanced Calculus for Applications*. 2nd ed. Englewood Cliffs, New Jersey: Prentice-Hall; 1976.